JOURNAL OF SOLID STATE CHEMISTRY **20**, 43–51 (1977)

A Study of Ti–O System between Ti_3O_5 and TiO_2 at High Temperature by Means of Electrical Resistivity

J. F. BAUMARD, D. PANIS, AND A. M. ANTHONY

Centre de Recherches sur la Physique des Hautes Températures, C.N.R.S., 45045 Orléans-Cédex, France

Received August 3, 1976

The Ti–O system between the compositions TiO_2 and Ti_3O_5 has been studied in following the electrical conductivity against the oxygen partial pressure. Several features are discussed: the dependence of electrical conductivity versus oxygen pressure, the kinetics of approach to equilibrium, and reversibility during oxidation and reduction paths. The results suggest an important contribution of point defects for small departures from the composition TiO_2 at high temperature.

Introduction

Nonstoichiometry in titanium dioxide, TiO_2 rutile, has been the subject of a number of investigations at high temperature. Such studies have been carried out mainly by means of electrical conductivity (*1–2*) and gravimetric analysis (*3*), as functions of temperature and oxygen pressure, and in electrochemical cells (*4*), where the metal/oxygen ratio was controlled by a dynamic oxygen pressure or by a coulometric titration. Results have been interpreted with a point defect model, the main justification of which was the ability to explain small departures from stoichiometry, as in many other oxides: NiO, CoO, . . . (*5*). Alternatively, authors claimed they found ionized oxygen vacancies or titanium interstitials, but it was generally accepted that the slope of the experimental isotherms was in favour of titanium interstitials (*2*).

For larger departures from the composition TiO_2, it is now well known, since the studies of Magneli and co-workers (*6*), and the numerous following structural results (*7*), that this oxide gives rise to homologous series, with ordered structures, the composition of which turns out to be Ti_nO_{2n-1}, derived from the rutile structure by a crystallographic operation called crystallographic shear (*CS*). This *CS* takes place on (121) planes for values of n between 4 and 10, or (132) planes for values of n between about 16 and 36, for samples prepared at 1273°K. Intermediate compositions between these two families are obtained by a progressive rotation of the shear planes, giving rise to new orientations, and accommodating by subtle steps increasing departures from stoichiometry (*7*). Thermodynamic investigations for large deviations from stoichiometry are rather poor. Electrochemical cells have been used by Valil'eva (*8*), and Suzuki (*9*). Stationary compositions are not always found for integral values of n. Anderson (*10*), and mainly Merritt (*11*), obtained a much higher precision in their gravimetric analysis. This last study shows a high density of data points, and it has been concluded that within the hysteresis loops occupied by the two *CS* planes families, stationary compositions exist. This is quite apparent for suboxides Ti_4O_7, Ti_5O_9, Ti_6O_{11}, and Ti_8O_{15}. However, the width of the hysteresis loops is generally larger than the variation of the oxygen chemical potential between two successive phases.

The electrical conductivity had been obtained in the range of oxygen pressure where the $\log \sigma$–$\log p_{O_2}$ plots are linear or quasilinear. They were interpreted with a point defect model. Electrical conductivity measurements are here extended to a larger oxygen pressure range, corresponding to compositions from TiO_2 to Ti_3O_5.

Experimental Procedure and Apparatus

The electrical conductivity has been measured by a 4 probe technique, according to Van Der Pauw (*12*). Samples used were monocrystalline disks; the geometrical axis is parallel to the *c* crystallographic axis. The sample dimensions are about 8 mm in diameter and 0.3 to 0.4 mm thick. A different sample was used for each isotherm.

Gas mixtures used to get oxygen partial pressures are of two kinds: CO–CO_2 and H_2–O_2–N_2. This last mixture fixes the oxygen chemical potential after combustion. The gas composition is obtained by appropriate mixing pumps. The variation in the composition of the gas buffer cannot be continuous. However, a great advantage is the good precision obtained on the ratio of the components (*2*).

The oxygen partial pressure has been calculated according to the available data of standard free energy for the formation of CO, CO_2, and H_2O. However, a problem remains concerning the choice of the data, owing to the scatter of the results found in the literature (*13–17*). At 1273°K, different available data are listed in Table I. The discrepancies are important, since differences for the molar free energy $\overline{\Delta G}_{O_2}$ are about 1200 cal $mole^{-1}$ at 1273°K for H_2–H_2O mixtures.

The lack of agreement between different authors concerning the suboxides stability as a function of oxygen pressure may probably be explained by this reason. The range of existence of a suboxide is in fact of the same order of magnitude as the discrepancy. We have chosen the data of Coughlin (*15*), because they give a reasonable mean value between the different data. Furthermore, there is a good agreement between the two sets of obtained data, as seen below.

The oxygen partial pressures have been verified with an electrochemical cell using calcia stabilized zirconia as a solid state electrolyte (*18*). Nernst law is well followed, even for high CO/CO_2 ratios, up to 99/1, in CO–CO_2 mixtures, within about 9 mV, taking the air as a reference. For H_2–H_2O mixtures, a deviation from the Nernst law is observed, although the order of magnitude of the experimental emf is right. This fact has received no satisfactory explanation, and was previously reported (*18*). The flow of the gas mixture was adjusted in such a manner that the emf of the cell did not depend on this flow.

Calculated conductivities are obtained with the initial geometrical dimensions of the sample. We suppose in a first approximation that the molar volume is not affected by the reduction.

Results

First we attempted to study the electrical conductivity during reduction at different temperatures, 1413, 1565, 1628, and 1693°K, in order to determine the kinetics of oxygen transfer between the solid and the gas phase. Some of these runs ended incidentally. Finally,

TABLE I

VALUES OF p_{O_2} CALCULATED ACCORDING TO THE DATA OF DIFFERENT AUTHORS AT 1273°K

	$CO + \frac{1}{2} O_2 \rightleftharpoons CO_2$ $CO/CO_2 = 1$		$H_2 + \frac{1}{2} O_2 \rightleftharpoons H_2O$ $H_2/H_2O = 1$	
Ref.	$-\log p_{O_2}$ (atm)	Dispersion $\overline{\Delta G_{O_2}}$	$-\log p_{O_2}$ (atm)	Dispersion $\overline{\Delta G_{O_2}}$
(*15*)	14.07	~600 cal $mole^{-1}$	14.57	~1200 cal $mole^{-1}$
(*14*)	14.00		14.36	
(*13*)	14.09		14.55	
(*16*)	14.11			
(*17*)			14.53	

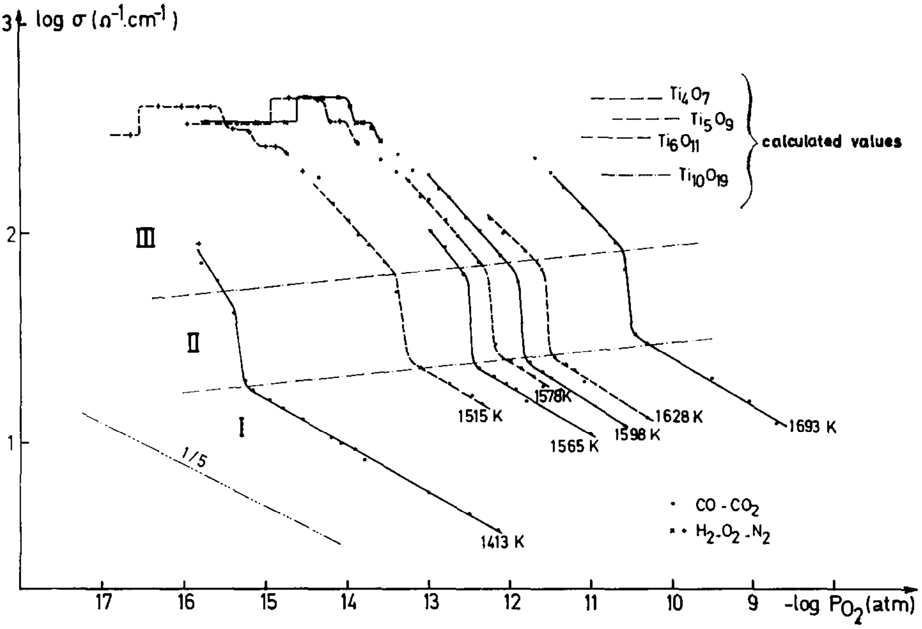

FIG. 1. A plot of electrical conductivity versus oxygen partial pressure at different temperatures.

three complete isotherms were obtained at 1515, 1578, and 1598°K (Fig. 1). The run at 1598°K also covered reoxidation (Fig. 2). The variation of electrical conductivity is the same at all temperatures; its dependence on oxygen chemical potential, the kinetics in the approach to equilibrium, and the hysteresis imply different areas I, II, and III (Fig. 1).

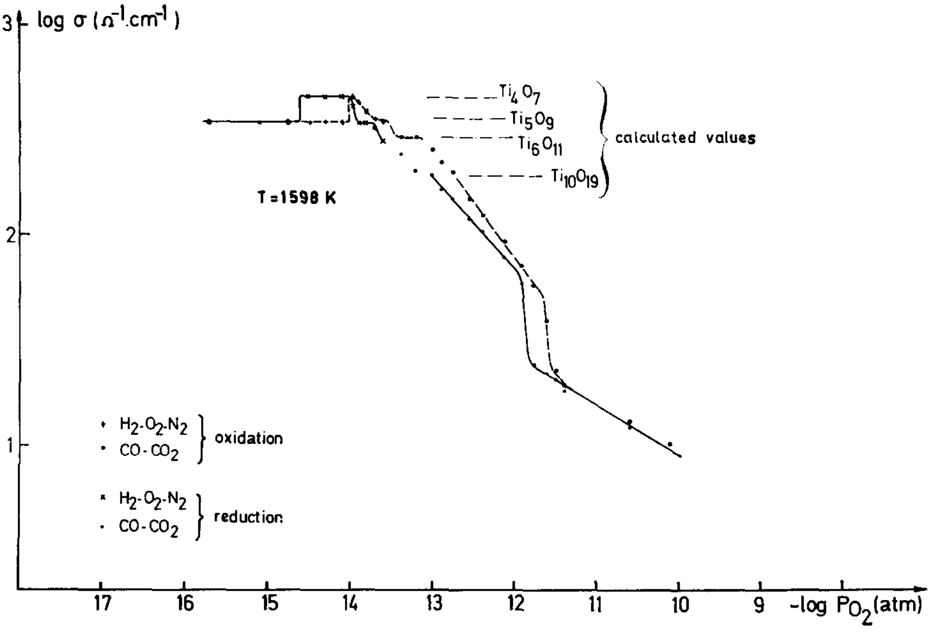

FIG. 2. A plot of electrical conductivity during oxidation and reduction paths at 1598°K.

Electrical Conductivity and the Nature of the Defects

In the area I, the plot of log σ against log p_{O_2} is linear, and a complete set of isotherms from 1273 to 1773°K has shown that the slopes were near $-1/5$ (*2*). So a simple interpretation based on a point defect model is readily suggested. The involved defects would be titanium interstitials $Ti_i^{4\cdot}$, taking the well-known analysis of Kröger and Vink:

$$Ti_{Ti}^{X} + 2\,O_0{}^{X} \rightleftharpoons Ti_i^{4\cdot} + 4e + O_2\,(g)$$
$$[Ti_i^{4\cdot}]\,[e]^4 p_{O_2} = K \qquad [e] = 4\,[Ti_i^{4\cdot}]$$
$$\sigma \alpha [e] \alpha p_{O_2}^{-1/5}$$

All the electrical conductivity measurements obtained by different authors are in good agreement. The limit of this high pressure area is $TiO_{1.990}$–$TiO_{1.992}$ at 1273°K. This limit does not seem to depend strongly on the temperature; it has been deduced from several kinds of measurements (*3*, *4*, *19*).

But the recent structural studies in the electron microscope, developed mainly by Bursill and Hyde (*7*), have shown that, even for very small departures from the stoichiometry, on quenched or slowly cooled down samples, the main defects were planar (132) defects, occurring by irregular *CS* planes in the rutile matrix. According to Hasiguti (*20*), these defects are present as soon as $x \simeq 0.0005$, i.e., for a concentration of defects of the same order of magnitude as the impurity concentration in good quality crystals. These extended defects are likely to exist at high temperature (*21*). The order observed in the electron microscope depends upon the preparation and approach to equilibrium at high temperature (*21*). Thus it was suggested that it was necessary to find another theoretical basis for the previous investigations which did not take the planar defects into account.

At the end of area I, one notices a rapid increase in the electrical conductivity, a factor of about 2.4 in magnitude. This variation is the same whatever the temperature may be (area II). At the end of the reduction process, the dependence of the electrical resistivity against the oxygen partial pressure becomes smaller and several stationary values appear, suggesting stationary compositions. The final product, identified by X-ray powder analysis after grinding is Ti_3O_5. So the different preceding phases are probably Magneli suboxides Ti_nO_{2n-1}, with $n = 4$, 5, and 6.

It is now well known that the compounds Ti_4O_7, Ti_5O_9, and Ti_6O_{11} present semiconductor-metal transitions in a temperature range much lower than this study (*22*). In a first approximation, we may assume one free electron per $3d^1$ titanium in these metallic oxides as in Ti_4O_7 (*23*). Assuming also that the electronic mobility is not strongly affected by the departure from stoichiometry, i.e., the number of crystallographic shear planes in the structure, we may calculate the electrical conductivities of Ti_5O_9, Ti_6O_{11} relative to Ti_4O_7. They are reported in Figs. 1 and 2. The agreement is good with the experimental data. The identification of the different phases after quenching was not used, since it has been reported to give mixtures, owing to the fact that the samples reoxidize rapidly as they cool down in the gas phase of the furnace (*7*).

The electrical conductivity of these suboxides Ti_4O_7, Ti_5O_9, and Ti_6O_{11} does not vary very much with temperature, as required by the metallic process of conduction in these compounds (*22*). Our data are in good agreement with the extrapolated results of Bartholomew on Ti_4O_7 and Ti_5O_9 single crystals at lower temperatures (*22*).

In the area I, taking a point defect model and assuming ionized titanium interstitials, the calculated mobility was near 0.17 cm^2 sec^{-1} V^{-1}.

The same electronic mobility is found if we suppose that main defects are (132) *CS* planes. If we assume that $Ti_i^{4\cdot}$ is the main defect:

in TiO_{2-x}:

$$x \simeq 2[Ti_i^{4\cdot}] = [e]/2 \qquad \text{since } x \ll 1.$$

If we assume (132) *CS* planes (the Ti_2O_3 notation must be taken in a formal sense):

$$TiO_{2-x} = (1-2x)TiO_2 + xTi_2O_3$$
$$x = \tfrac{1}{2}[Ti\,3d^1] = [e]/2.$$

The same relation exists between electronic concentration and composition. Here, [ ] denotes the molar fraction expressed by the ratio of the number of considered species to the number of TiO_2 molecules. Thus the calculated mobility is independent of the model. In the case of Ti_4O_7, this mobility turns out to be equal to 0.17 $cm^2 sec^{-1} V^{-1}$, indicating that it probably does not change with the departure from stoichiometry. The variation of electrical conductivity in the area II is the same for all the isotherms, e.g., a factor 2.4. For instance at 1273°K, if the composition of the sample was close to $TiO_{1.992}$ at the boundary of area I, it changes rapidly to $TiO_{1.973}$, corresponding to the upper limit of (132) *CS* planes family compounds. This rapid increase suggests a diphasic system, as was reported by several authors (*11*, *19*). The texture would then consist of more or less dispersed *CS* planes within a rutile matrix. The rutile phase saturated with extended defects is in equilibrium with the highest ordered phase Ti_nO_{2n-1}. Another point of view will be given later.

The following area III would then be occupied by the (132) *CS* planes family Ti_nO_{2n-1}. It is not possible with our apparatus to discern adjacent stationary compositions. The variation in the departure from stoichiometry and in the number of available carriers is too small. The same thing is true for (121) structures when $n \gtrsim 7$. The range of intermediate compositions between the two families varies with temperature (*7*). An order of magnitude may however be deduced from the resistivity of $Ti_{10}O_{19}$, as calculated and reported on Fig. 1.

The Approach to Equilibrium and its Kinetics

In area I, evolution of the solid after a change in the composition of the gas phase is very rapid, of the order of minutes, from 1273 to 1773°K (*2*). Subsequent measurements of chemical diffusion coefficient of oxygen (*24*), analyzed in a classical model (*25*) involving point defects, indicate a very high value for this coefficient, about 10^{-4} $cm^2 sec^{-1}$ around 1500°K, and this coefficient is independent of the composition at constant temperature, within experimental error. The oxygen transfer between the solid and the gas buffer becomes suddenly much slower in areas II and III. The experimental results can no more be fitted by a classical model. However, we can deduce that the chemical diffusion coefficient of oxygen drops by about four orders of magnitude at the boundary of area I.

The influence of temperature on the approach to equilibrium in the domain of Ti_nO_{2n-1} suboxides has been discussed by several authors around 1273°K. According to Anderson (*10*), nonequilibrium was not a problem beyond 1323°K. On the other hand,

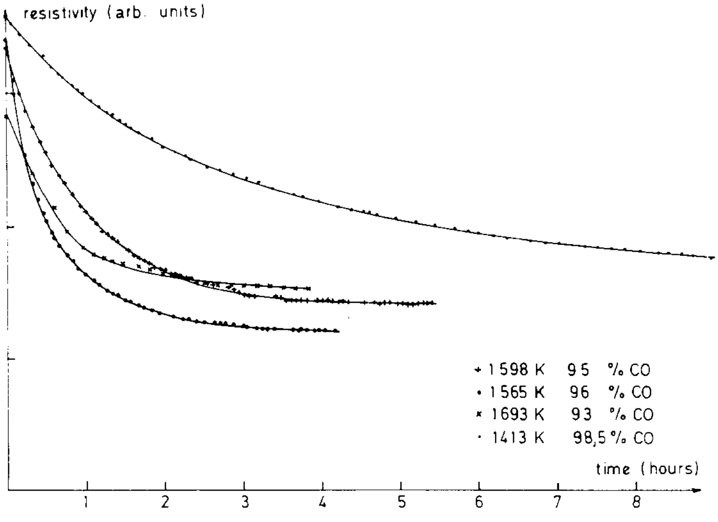

FIG. 3. The effect of temperature on kinetics of oxygen transfer between the solid and the gas phase.

Merritt and Hyde (*11*) think that true equilibrium is rarely obtained, and in their experiments they observed weight changes often 36 hours after a change in the oxygen chemical potential. They estimated that the kinetics were not greatly affected by temperature. Therefore, some preliminary measurements were undertaken to clarify this situation. Curves of resistivity as a function of time for the same transition through the area II are plotted in Fig. 3 at different temperatures. The effect of the temperature is quite evident.

The kinetics may however vary a little in area III with the composition of the sample. According to the data obtained at 1598°K, they are about the same during reduction and reoxidation. The end of evolution of the solid was assumed to be reached, when, after about 2 hours, the variation of conductivity was lower than the sensitivity of our apparatus. The study at 1413°K was not carried out because the reaction rate was too slow and the measurements were made beyond 1500°K. The last run at 1598°K lasted one month.

The reaction was rapid only at the transformations Ti_4O_7–Ti_3O_5. They took about one hour after an induction period.

Hysteresis

In area I, the data obtained during reduction and oxidation are reversible within experimental error (*2*). When one gets larger departures from stoichiometry, an hysteresis loop is observed. However, always in area I, the data are the same within experimental error during reduction and reoxidation.

The monocrystalline state of the sample is destroyed during the reduction, especially after transitions between Ti_4O_7 and Ti_3O_5. A small anisotropy has been reported in the conductivity of reduced rutile TiO_{2-x}; this latter is higher in the direction of c crystallographic axis, by a factor between 1 and 3 (*1*), and the same order of magnitude has been reported for Ti_4O_7 (*22*). However, the values obtained for Ti_4O_7, Ti_5O_9, and TiO_{2-x} (for $p_{O_2} \gtrsim 10^{-14}$ atm) are the same, suggesting a small, if any, contribution of anisotropy to the hysteresis loop. Thus hysteresis is present, as in the study of Merritt (*11*), even at temperatures higher than 1300°K. The loop is quite pronounced for the transformation Ti_4O_7–Ti_3O_5–Ti_4O_7 (about 4 kcal $mole^{-1}$).

Hysteresis has been attributed to the excess chemical potential necessary to generate a new *CS* plane (*7*). This is compatible with the fact that an extended defect rarely ends within a crystal and this implies a high energy for the dislocation bounding the defect. So the question arises whether irregular *CS* planes are the main defects for small deviations from stoichiometry, since no hysteresis is observed in area I.

Discussion

All these different properties suggest that, even if the experimental situation is relatively clear for suboxides of the (121) and (132) families, where the existence of stationary compositions are demonstrated by the gravimetric analysis of Merritt (*11*), the behavior of the oxide is not so simple in the range $TiO_{1.97}$–TiO_2, in areas I and II.

Observations in the electron microscope strongly support the presence of extended defects for very small departures from stoichiometry, as low as 10^{-3}–10^{-4}. If we admit the presence of these extended defects in all the range of oxygen pressure, it becomes necessary to explain the differences observed in the variation of electrical conductivity, chemical diffusion coefficient, and hysteresis. Unhappily, no theoretical thermodynamic data is available concerning the dependence of composition as a function of oxygen molar free energy $\overline{\Delta G}_{O_2}$ for these suboxides derived from a parent structure by a *CS* operation. A qualitative interpretation for the diphasic gap would be based on the interaction potential energy between two isolated shear planes. A simple curve giving the form of this potential has been proposed by Bursill and Hyde (*22*). A striking feature is the presence of long range forces, up to 200 Å about. This is of the order of magnitude of the distance between *CS* planes if we assume that planar defects were perfectly organized in the matrix at the composition $TiO_{1.99}$. At these distances, the interaction is essentially attractive; the nucleation energy for a new extended defect would be somewhat reduced and one waits for a larger dependence of composition against $\overline{\Delta G}_{O_2}$. However, this hypothesis is not very attractive, because interaction probably leads to a more progressive variation, as interaction between point defects in oxides (*27*). Hysteresis, as we have seen, has been attributed to excess $\overline{\Delta G}_{O_2}$ necessary to generate a new *CS* plane. The absence of hysteresis in area I is then striking, if one admits the presence of extended defects. Similarly it is difficult to understand the abrupt variation in the chemical diffusivity coefficient of oxygen at the boundary of area I, even if a strong interaction between planar defects implies local reorientation and lateral migration of the defects, the mechanism of which would constitute the limiting step in the evolution of the crystal.

Another point of view is to admit the presence of point defects in area I at high temperature. The behavior of the oxide is similar to what we then expect from a theoretical model. The usual dependence of electrical conductivity and composition against $\overline{\Delta G}_{O_2}$, the reversibility or absence of hysteresis, the evolution of electrical conductivity with time during chemical diffusivity measurements, the relation between chemical diffusivity and tracer diffusion experiments are then well understood. The molar partial mixing enthalpy of oxygen remains a constant at 1323°K between the compositions TiO_2 and $TiO_{1.995}$ (*3*), then increases a little up to $TiO_{1.990}$; that indicates that for departures from stoichiometry up to 0.005, mass action law is valid for concentrations of point defects and associated species. Beyond this composition, there is some interaction between point defects. In area II, one should have a diphasic system between rutile with point defects and the highest ordered phase Ti_nO_{2n-1} of the (132) family. One notices a small variation of the electrical conductivity at the boundary of area I with temperature. This should indicate either a small change in electronic mobility or a change in the compositions limiting the diphasic gap. The first hypothesis is less probable, for it has been shown that the Hall mobility is a decreasing function of temperature (*27*). Thus the extent of area I increases somewhat with temperature and the upper limit of (132) *CS* phases decreases in the same time. The situation is depicted schematically in a diagram showing the mixing free energy as a function of composition in Fig. 4. The only problem remains to explain why even if the homogeneity range of rutile is very small at room temperature, planar defects are observed in the electron microscope on

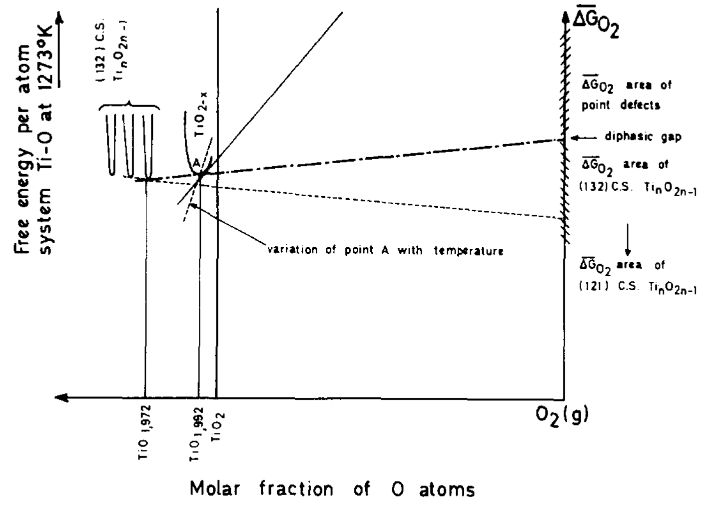

FIG. 4. A schematic diagram showing the free energy per at.g in the system Ti–O at 1273°K (for clarity of the drawing, the oxygen chemical potential is depicted lower than given according to the experimental data).

quenched samples. That seems to be in contradiction with the relatively low mobility of oxygen in the (121) or (132) *CS* planes compounds. However, the high value of chemical diffusivity in area I, indicative of a great mobility of point defects does not exclude some organization as the sample cools down, and the homogeneous range of rutile decreases.

Thermodynamic Data

In the range where hysteresis is present, the variation of $\overline{\Delta G_{O_2}}$ between two successive phases is often smaller or of the same order of magnitude as the width of the loop. Moreover (cf. Fig. 2), for compositions which do not correspond to integral values of n, hybrid structures may exist (*7*). So transitions are not abrupt, except for Ti_4O_7–Ti_3O_5, where they are complete after an induction period. That prevents from getting a good thermodynamic information on the stability of the different phases. In our range of temperature, the only available data have been published by Suzuki and Sanbongi (*9*). They are compared with our results in Table II. Our data are also in good agreement with those obtained by Zador and Alcock (*28*). That gives further validity to identification of the different phases as was done previously.

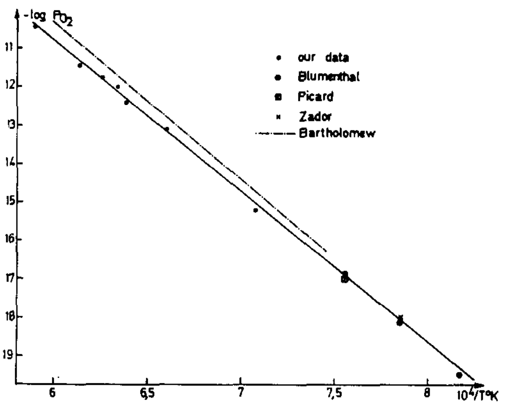

FIG. 5. The limit of the area of homogeneous rutile, versus temperature and oxygen partial pressure, compared with the data of Blumenthal (*19*), Picard (*3*), Zador (*4*), and Bartholomew (*29*).

On Fig. 5, is plotted the boundary of area I during reduction, which has been called the domain of homogeneous rutile. Our results are in good agreement with the results of Blumenthal (*19*) and are at lower pressures than those of Bartholomew (*29*). We may also notice that the thermodynamic properties are not affected by the nature of the gas buffer, at least for large departures from the composition TiO_2. The results obtained with CO–CO_2 and H_2–H_2O buffers are consistent.

Conclusion

The main results obtained for large departures from stoichiometry are also found by means of electrical conductivity. However, this method clearly shows the difference between small departures from stoichiometry and the compositions corresponding to ordered or quasiordered Ti_nO_{2n-1} phases. It is obviously not necessary to recall that the published structural studies are made on quenched samples and that thermodynamic studies are made in situ. To explain the different properties of nonstoichiometric rutile, we assume a

TABLE II

VALUE OF $\overline{\Delta G_{O_2}}$ FOR THE TRANSITIONS BETWEEN THE DIFFERENT PHASES (kcal mole^{-1}) AT 1598°K (VALUES OF SUZUKI AND ALCOCK EXTRAPOLATED AT 1598°K)

Transition	Our results		Suzuki (*9*)	Alcock (*28*)
	Reduction	Oxidation		
Ti_6O_{11}–Ti_5O_9	99.8	98.7	99.4	98.3
Ti_5O_9–Ti_4O_7	102.0	101.2	101.2	101.2
Ti_4O_7–Ti_3O_5	107.1	102.7	105.3	104.2

range of existence of point defects at high temperature, where the behavior of the oxide is quite different. Especially, the high mobility of oxygen near the composition TiO_2 seems to be indicative of the important role of point defects. This range of homogeneous rutile strongly decreases with temperature, since extended defects are found at room temperature or near room temperature in electron microscopy. Finally, one should have an equilibrium between TiO_{2-x} and the highest ordered phase Ti_nO_{2n-1}, for larger departures from stoichiometry, before the apparition of suboxides Ti_nO_{2n-1} of the (132) family, at high temperature.

References

1. R. N. Blumenthal, J. Baukus, and W. M. Hirthe, *J. Electrochem. Soc.* **114**, 172 (1967).
2. J. F. Baumard, D. Panis, and D. Ruffier, *Rev. Int. Htes Temp. Refract.* **12**, 321 (1975).
3. C. Picard, Thesis, Paris, 1974.
   C. Picard and P. Gerdanian, *J. Solid State Chem.* **14**, 66 (1975).
4. S. Zador, *in* "Electromotive Force Measurements in High Temperature Systems," The Institution of Mining and Metallurgy, London (1968).
5. For example, "Electrical Conductivity in Ceramics and Glass" (N. M. Tallan, Ed.), Part A, Dekker, New York (1974).
6. S. Andersson, B. Collen, U. Kuylenstierna, and A. Magneli, *Acta Chem. Scand.* **11**, 1641 (1957).
7. L. A. Bursill and B. G. Hyde, *in* "Progress in Solid State Chemistry," Vol. 7 (Reiss and MacCaldin, Eds.), Pergamon, London (1972).
8. I. A. Vasil'eva and E. Y. Shaulova, *Russ. J. Inorg. Chem.* **43**, 1713 (1969).
9. K. Suzuki and K. Sanbongi, *Tetsu-to-Hagané* **58**, 1579 (1972). Translated in *Trans. Iron and Steel Inst. Japan* **15**, 619 (1975).
10. J. S. Anderson and A. S. Khan, *J. Less Common Metals* **22**, 219 (1970).
11. R. R. Merritt and B. G. Hyde, *Phil. Trans. Roy. Soc. London, Ser. A* **274**, 627 (1973).
12. L. J. van der Pauw, *Philips Research Reports* **16**, 187 (1961).
13. J. F. Elliott and M. Gleiser, *in* "Thermochemistry for Steelmaking," Addison–Wesley, London (1960).
14. C. E. Wicks and F. E. Block, Bull. 605 of the Bureau of Mines (1963).
15. J. P. Coughlin, Bull. 542 of the Bureau of Mines (1954).
16. O. Kubachewski, E. L. Evans, and C. B. Alcock, "Metallurgical Thermochemistry," 4th ed. Pergamon, London (1967).
17. JANAF Thermochemical Tables, 2nd edit., U.S. Department of Commerce, N.B.S. (1971).
18. T. H. Etsell and S. N. Flengas, *Met. Trans.* **3**, 27 (1972).
19. R. N. Blumenthal and D. H. Whitmore, *J. Electrochem. Soc.* **110**, 92 (1963).
20. R. R. Hasiguti, *Annual Rev. Mat. Sci.* **2**, 69 (1972).
21. L. A. Bursill and B. G. Hyde, *Phil. Mag.* **23**, 3 (1971).
22. R. F. Bartholomew and R. D. Frankl, *Phys. Rev. B* **187**, 828 (1969).
23. M. Marezio and P. D. Dernier, *J. Solid State Chem.* **3**, 340 (1972).
24. J. F. Baumard, to be published.
25. L. W. Laub and J. B. Wagner, *Oxidation of Metals* **9**, 29 (1975).
26. R. N. Blumenthal, P. W. Lee, and R. J. Panlener, *J. Electrochem. Soc.* **118**, 123 (1971).
27. I. Branski and D. S. Tannhauser, *Solid State Commun.* **7**, 245 (1969).
28. C. B. Alcock, private communication.
29. R. F. Bartholomew and W. B. White, *J. Crystal Growth* **6**, 249 (1972).